

**BABEȘ – BOLYAI UNIVERSITY**  
**FACULTY OF PHYSICS**

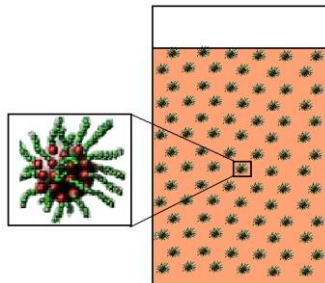
**CHIORAN VIORICA**

**STUDY OF THE PHYSICAL PROPERTIES OF SOME  
MAGNETIC NANOFUIDS**

**PhD Thesis Summary**

**Scientific supervisor**

**Prof.Univ.Dr. IOAN ARDELEAN**



**CLUJ – NAPOCA**

**2014**

**- 1 -**

## **Abstract**

This paper studied the physical properties (magnetic, structural, dielectric, optical, thermal, rheological) of some magnetic nanofluids. For this purpose three samples of magnetic nanofluids called L1, L2 and L3 were prepared. They contain magnetite particles stabilized with oleic acid and dispersed in the petroleum and kerosene.

Four types of measurements were conducted using high performance technology: the VSM 880 magnetometer, Philips CM 120 Microscope (TEM), Physica MCR 300 rheometer.

The following aspects were analyzed: preparation methods, quality of the obtained samples, superparamagnetic behavior, stability of the nanofluids in physical fields (electric and magnetic), rheological behavior and possible applications.

**Keywords:** magnetic nanofluids, magnetization, magnetic susceptibility, superparamagnetic.

# CONTENTS

<b>Introduction</b> .....	1
<b>Chapter 1. Study on magnetic materials</b> .....	3
1.1. The magnetization of magnetic materials .....	3
1.1.1. The interaction between magnetic field and magnetic material .....	3
1.1.2. Forces acting on particles with magnetic moment.....	7
1.1.3. Spontaneous domain magnetization theory ( Weiss domains) .....	8
References.....	12
<b>Chapter 2. Magnetic nanofluid's preparation and properties</b> ...13	
2.1. Methods of obtaining magnetic nanoparticles .....	13
2.1.1. Dispersion method.....	14
2.1.2. Chemical condensation method .....	16
2.2. Methods of obtaining magnetic nanofluids .....	17
2.2.1. The mechanical dispersion method .....	18
2.2.2. Electro-condensation method .....	20
2.2.3. Thermal degradation method .....	21
2.2.4. Electro-deposition method .....	22
2.2.5. Chemical precipitation method .....	23
2.2.6. The change of nanofluid base .....	24
2.3. Physical properties of magnetic nanofluids .....	25
2.3.1. Magnetic, electrical and dielectric properties.....	25
2.3.2. Rheological properties .....	28
2.3.3. Thermal properties .....	31
2.3.4. Optical properties .....	31
2.3.5. Conversion parameter of the magnetic properties .....	32
2.4. Analysis methods of the physical properties of magnetic nanofluids .....	36
2.4.1. Analysis of the magnetization curves .....	36
2.4.2. Analysis of the magnetic nanofluid's stability in physic fields .....	40
2.4.3. Analysis methods based on the electron microscope technique .....	45
References .....	47

<b>Chapter 3. Experimental techniques used in this paper</b> .....	49
3.1. Obtaining and preparing the samples .....	49
3.1.1. Obtaining the magnetic nanofluid samples .....	49
3.1.2. Methods of improving the sample's quality .....	56
3.1.3. Preparing the magnetic nanofluid samples .....	58
3.2. Measurement techniques .....	60
3.2.1. Electron microscope measurements .....	60
3.2.2. Magnetic measurements by Gouy's method .....	63
3.2.3. Measurements using VSM880 magnetometer .....	64
3.2.4. Measurements using Physica MCR 300 rheometer .....	66
References .....	69
<b>Chapter 4. Results and discussions</b> .....	71
4.1. Study on the quality of the samples .....	71
4.1.1. Microstructure and dimensional distribution analysis of the magnetite particles .....	71
4.1.2. Study of the conversion parameter of the magnetic properties.....	83
4.1.3. Study of the magnetic properties using the magnetization curve analysis .....	94
4.1.4. The magnetic material influence on the magnetic field lines.....	104
4.1.5. Elements that influence the magnetization process and limit the saturation magnetization .....	106
4.1.6. Magnetic susceptibility determination using Gouy's Method.....	107
4.2. Study of the stability of magnetic nanofluids placed in physical fields .....	110
4.2.1. The stability of nanofluids in gravitational field.....	110
4.2.2. The stability of nanofluids in magnetic field .....	116
4.2.3. The influence of temperature on the stability of nanofluids in gravitational field .....	121
4.3. Viscosity study on magnetic nanofluids in the absence of magnetic fields .....	128
4.4. Possible uses of magnetic nanofluids.....	133
References .....	138
<b>Conclusions</b> .....	143

## INTRODUCTION

Magnetic nanofluids formed as biphasic colloidal suspensions, obtained through specific chemical processes and techniques, are particularly interesting for study because their physical properties recommend them to be used successfully in a wide range of scientific and biomedical purposes, as well as in modern technologic applications.

This paper's goal is to conduct a thorough study of the physical properties of some magnetic nanofluids. Achieving this goal requires achieving other specific objectives first, namely: magnetic nanofluid sample preparation, magnetic nanofluid sample quality check, a study of the sample's physical properties (structural, magnetic, rheological and thermal), stability analysis of the sample in gravitational and magnetic fields, identifying possible applications for the studied nanofluids.

Weiss domain spontaneous magnetization theory as well as some aspects of the interaction between the magnetic field and the material with magnetic properties, were both considered, then we took from the scientific literature and analyzed known methods for obtaining mono-domain particles and for the preparation of magnetic nanofluids.

After a brief overview of the magnetic nanofluid's main physical properties (magnetic, electrical, dielectric, rheological, thermal and optical), we describe the experimental method used to obtain the samples, the techniques used to improve their quality and measurement techniques.

Four types of measurements were performed using high performance devices such as: VSM 880 vibrating sample magnetometer used for magnetic measurements, Physica MCR 300 rheometer used for rheological measurements and for measurements by electron microscopy the CM 120 (TEM) electron microscope was used.

The last chapter contains the experimental results and their interpretation obtained after studying the magnetic nanofluids.

Closing the paper are the main clear and concise findings, drawn from the studies and work conducted during the preparation of this PhD thesis. These findings have been published (or, are to be

published) both in national and international magazines and have been presented at conferences and scientific symposiums in Romania and abroad.

## **Chapter 1. The magnetization of magnetic materials**

Current theories on magnetic phenomena have as starting point Ampere's hypothesis on molecular currents, stating that magnetism has its origins in the circular atomic currents that exist within all materials. The magnetic properties of the magnetic materials are based on the magnetic dipoles that appear in the material's structure [1].

Atoms are characterized by an elementary magnetic moment ( $\vec{\mu}$ ) determined as the vectorial sum of the elementary magnetic moments of the dipoles contained within the atom [2]. When applying a  $\vec{H}_0$  intensity magnetic field on the magnetic material, the elementary magnetic moments tend to orient themselves in the direction of the field lines [3]. This phenomenon is known as the material's magnetization and the magnetic susceptibility ( $\chi$ ) is a measure of the magnetic material's ability to magnetize [4].

To explain the fact that within ferromagnetic materials a non-zero magnetization can exist even in the absence of an external magnetic field, Weiss [5] made the assumption that below the Curie temperature ( $T_c$ ), a ferromagnetic material is magnetized to saturation on microscopic regions within which the permanent magnetic moments spontaneously order themselves in a direction coinciding with the direction of light magnetization [6].

Weiss's theory clarifies that ferromagnetic properties exist because of the electron spin magnetic moments and their orientation is due to a purely quantum effect called the exchange effect [7].

The exchange magnetic forces have a short action range and align the spins while the classic magnetic forces act over long range and tend to orient the elementary magnetic moments in opposite directions so the North Pole of a tiny magnet is next to the South Pole of a neighbor and parallel magnet [8].

## Chapter 2. Magnetic nanofluid's preparation and properties

Magnetic nanofluids, also known as nanofluids, magnetic fluids or magnetic liquids are a special class of nano materials having simultaneously the properties of a typical liquid and those of a magnet [9]. They are two-phase environments composed of ferromagnetic / ferrimagnetic or paramagnetic colloidal particles suspended in a liquid base [10]. The number of dispersed particles is very high, around  $10^{23}$  particles per cubic meter to enable the expression of the magnetic forces in the liquid [11]. In order to be uniformly dispersed and to have the necessary magnetic properties, the particles should have dimensions comparable to a critical size, below which the mono-domain structure appears.  $R_{cr}$  - the critical radius corresponding to the transition from a multi-domain to a mono-domain structure ranges from 14nm to 17nm , for spherical or sharp iron particles [12].

The preparation process of a magnetic nanofluid involves two important steps: obtaining very fine magnetic particles and stabilizing the colloidal suspensions [13].

The most commonly used methods to obtain mono-domain colloidal particles are: the dispersion method and the chemical condensation method [14]. The chemical processes developed for the synthesis and dispersion of magnetic nanoparticles in various polar and non-polar base liquids, use steric stabilization methods that can be monolayer, two-layer or mixed (steric-electrostatic) to prevent the agglomeration and sedimentation of nanoparticles [15].

To successfully obtain magnetic nanofluids the following methods are used: the mechanical dispersion method, the electro-condensation method, the thermal dissolution method, the electro-deposition method, the chemical precipitation method and the change of nanofluid base [16-18]. Physical methods for obtaining ferromagnetic particles (Fe, Co) were also considered through thermal plasma technologies aimed at obtaining highly magnetized magnetic nanofluids and magneto-rheological suspensions [19, 20].

Magnetic nanofluids have very special physical properties that are highlighted in the interaction with a magnetic field. They respond almost instantly by flowing, levitating, repositioning or by changing the internal pressure's spatial distribution; through the

action of a magnetic field on a magnetic nanofluid, the spontaneous formation of high stability peaks occurs, an amount of magnetic nanofluid may levitate in space, a permanent magnet within the magnetic nanofluid may also levitate and a non-magnetic object immersed inside the magnetic nanofluid undergoes a stable levitation. It has no hysteresis [21-28].

### **Chapter 3. Experimental techniques used in this paper**

In order to study the physical properties of magnetic fluids, three samples referred as L1, L2 and L3 have been prepared in the laboratory then analyzed and compared in the course of this study. All the samples contain magnetite nanoparticles ( $\text{Fe}_3\text{O}_4$ ) stabilized with oleic acid ( $\text{C}_{18}\text{H}_{34}\text{O}_2$ ) and dispersed in hydrocarbons (L1 and L3 samples are dispersed in petroleum and L2 sample is dispersed in kerosene) [29].

One of the methods used to prepare the magnetic nanofluids necessary to our proposed experimental research was the chemical precipitation method, which has been improved so as to obtain nanofluids that have the required quality [30-32].

The main reason for choosing this method was the considerable reduction in the time needed for obtaining the final product [33-41]. The methods used in the magnetic nanofluid preparation process for improving their quality, involves efficient stabilization techniques, the separation and filtration in high gradient magnetic field and sample ultracentrifugation [42-47].

Using high performance devices, four types of measurements were conducted on our magnetic nanofluid samples.

The structural morphology of our magnetic nanofluid samples was analyzed using transmission electron microscopy technique (TEM). The measurements were performed using a Philips CM-120 (TEM) electron microscope. The working parameters used are as follows : electron acceleration voltage  $U = 100$  kV, the wavelength of the emitted electrons  $\lambda = 0,037$  Å and the resolution  $\pm 2$  Å. The TEM electron microscope uses a beam of electrons accelerated to energies ranging between 40 - 100 keV, focused by a series of magnetic lenses and transmitted through the sample. The electron beam leaving the sample contains information about the analyzed material [48].

We obtained this way, for the studied magnetic nanofluid samples, diffraction diagrams, histograms, particle distribution curves based on diameters and diffraction images [49-51].

The magnetometer and granulo-magnetometer measurements were conducted using type VSM 880 magnetometer. The magnetization curves for L1, L2 and L3 samples have been determined. A magnetic description of the magnetic nanofluid samples with polydisperse magnetite particles having a lognormal distribution was performed. The dimensional distribution parameters were determined : the average magnetic diameter ( $D_m$ ), standard deviation ( $\sigma_m$ ), saturation magnetization ( $M_s$ ) and the initial magnetic susceptibility( $\chi_i$ ).

The system used for measurements by Gouy method comprises of an electromagnet with cylindrical pole pieces, a rheostat, a microscale and one tesla-meter [52]. The studied sample is placed in a test tube having the section (S) and length (l), placed on a microscale located in the air gap of the electromagnet that provides a magnetic field with ( $\vec{B}$ ) magnetic induction and ( $\vec{H}$ ) intensity, perpendicular to the sample. Using a rheostat to change the current intensity (I), a variation in magnetic field strength and induction is caused. A tesla-meter shows the magnetic induction's values. An apparent increase in the sample's weight is caused and the apparent increase in the sample's mass ( $\Delta m$ ) is measured using the microscale. The initial magnetic susceptibility  $\chi_i$  and saturation magnetization ( $M_s$ ) are determined based on experimental data [53].

The magnetic nanofluid's rheological / magneto rheological behavior was evaluated using a Physica MCR 300 rheometer.

For the analyzed samples we measured and evaluated the following: dynamic viscosity, complex viscosity, shear stress, the loss angle tangent, magnetic viscosity, kinematic viscosity, temperature, rotation speed, shear speed, frequency, angular velocity and reorientation time [54]. MCR 300 magnetometer has specialized software for measurements managing and processing experimental data.

## Chapter 4. Results and discussions

The last chapter of the thesis presents the results obtained after studies and measurements of the L1, L2 and L3 magnetic nanofluid samples were conducted.

### 4.1. Study on the quality of the samples

#### 4.1.1. Microstructure and dimensional distribution analysis of the magnetite particles

Experimental measurements were made with Philips CM-120 (TEM) microscope which allows the study of particle microstructure through electron diffraction on crystals.

The experimental data obtained for samples L1, L2 and L3 were simultaneously analyzed in order to make a comparative study.

*a) Analyzing magnetite nanoparticles by electron microscopy* we tried to highlight the internal structure of magnetite ( $\text{Fe}_3\text{O}_4$ ) as well as the shape and size of nanoparticles and homogeneity of the mixture of nanoparticles.

After studying the diffraction images corresponding to samples L1, L2 and L3, we noted very similar characteristics regarding the polycrystalline structure confirmed by the presence of diffraction rings and a high crystallinity confirmed by the presence of spots in the narrowed diffraction rings.

The electron's diffraction images on magnetite particle crystals were taken from areas where diameters have been determined, to make a complete structural analysis of the samples.

Diffraction rings were formed when electrons accelerated to 100 kV and a wavelength  $\lambda = 0.037 \text{ \AA}$  pass between the atoms of the crystalline magnetite network having the constant  $a=0.839 \text{ nm}$ .

Since diffraction rings alternate with dark areas (wider for L3 sample), the existence of clusters of particles that cause inelastic collisions can be admitted. These collisions are followed by the accelerated electron's loss of energy or they may be scattered by very large angles.

Using diffraction rings we know the electrons density distribution in the studied material, so we can analyze the cubic

crystalline structure of magnetite ( network constant, any defects in the crystal, the crystallinity of analyzed samples) [55-57].

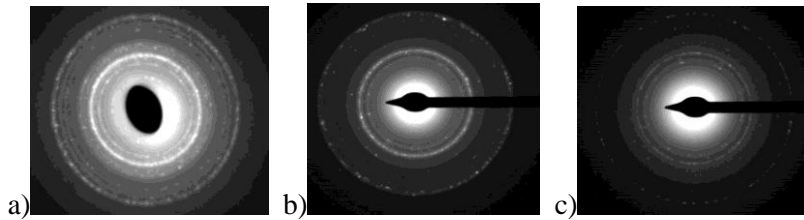


Fig.4.1. Diffraction rings obtained for our nanofluid samples L1 (a), L2 (b) și L3 (c).

In the center of the diffraction image fig.4.1 the Airy disk can be seen, representing the smallest area where the spot of not diverted electrons passing through the magnetite’s crystal structure could be located.

*b) Sample description by analyzing the electron micrographs* shown in fin.4.2 indicates a fractal, chain and mixed agglomeration tendency of magnetic particles. The groups of particles uniformly dispersed do not form clusters and form a homogeneous mixture.

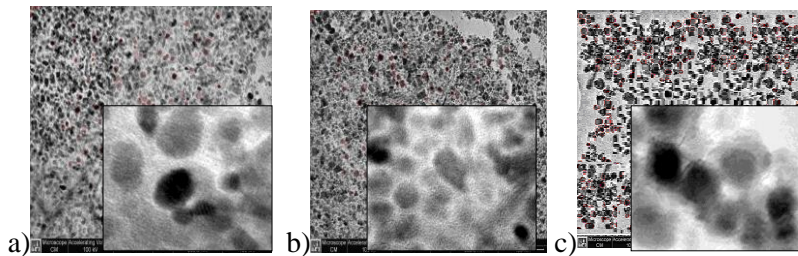


Fig.4.2. Electron micrographs for samples L1(a), L2(b) și L3(c).

The study of micrographs reveals that the analyzed samples are composed of magnetite nanoparticles quasi-static in shape, size close to ( $10^{-9}$ m) and a composed structure type core-shell.

The core has darker contrast than the (amorphous) structure covering it. It consists of a mono-domain crystal with interplanar distances of 2.1Å and 2.2 Å, specific to metallic iron. The shell

consists of layers spaced at 3.6 Å. The electron diffraction indicates the presence of α-Fe phase with rings that correspond to the interplanar distances (110) and (211) – (the partial oxidation of iron in the non-magnetic layer).

*c) Characterization of samples by analyzing histograms and distribution curves of particles, based on diameter length.*

Figure 4.3.a shows the distribution curve based on particle diameters in L1 sample and the histogram that shows A = 27.0927 % the maximum frequency of occurrence of d=9.984nm physical diameter particles. L1 sample contains magnetic particles with an average diameter size of  $\bar{d}_1 = 10.99nm$ .

Figure 4.3.b shows the diameter based distribution. This distribution covers on the graphic a “zone” between (8-14nm). We notice some very large diameters while the very small ones are insignificant.

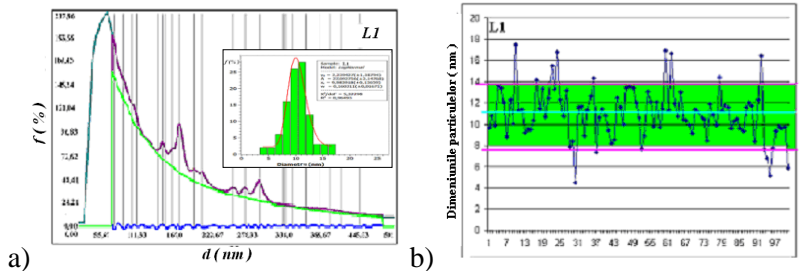


Fig. 4.3.a) Distribution curve based on diameter and histogram  
 b) Distribution based on sample L1’s particle diameter

For dimension estimates we used the Lognormal function (red curve in fig.4.3.a). We can observe the Gaussian type shape of the diameter based distribution curve of the magnetite particles, for all the analyzed samples (L1, L2 and L3).

The (minimum) magnetic diameters obtained by fitting the distribution curves with Log-normal functions have these values:  $d_1 = 3.07 nm$  (L1),  $d_2 = 2.943 nm$  (L2) and  $d_3 = 2.941 nm$  (L3).

We observe similar characteristics for the histograms of the samples: a wide range of diameter values is indicated by the dispersion while the standard deviation shows the diameter’s

deviation from the average diameter. The asymmetry coefficient indicates an asymmetry to the right and the excess factor value indicates a higher vaulting [58-64].

Parameter values determined from the statistical processing of the experimental data are shown in Table 4.1.

*d) Description of samples based on statistical analysis of experimental data.*

Table 4.1. Parameters describing the microstructure and particle diameter distribution of samples L1, L2 and L3.

No. of particles 100	Sample L1	Sample L2	Sample L3
Minimum diameter	4.52	5.17	3.34
Average diameter	10.99	10.51	8.70
Maximum diameter	17.51	19.61	16.91
Standard deviation	2.40	2.44	2.61
Excess factor	0.68	1.57	0.46
Asymmetry	0.24	0.81	0.75
Dispersion	5.74	5.95	6.83

#### **4.1.2. Study on the conversion parameter of the magnetic properties**

The conversion parameter of the magnetic properties ( $\gamma$ ) is of practical importance because it describes the quality of magnetic fluids with technological applications [65].

In a first step we determined the values of the solid volume fraction ( $\varepsilon_s$ ) and of the magnetic volume fraction ( $\varepsilon_M$ ), then we determined the conversion parameter of the magnetic properties ( $\gamma$ ) using several calculation methods [66].

In order to calculate the magnetic volume fraction we determined the saturation magnetization ( $M_s$ ) using a vibrating sample magnetometer. To calculate the solid volume fraction we performed density measurements using pycnometer method. The calculated values of the conversion parameter are presented in Table 4.2.

Table 4.2. The calculated values of the conversion parameter of the magnetic properties.

Sample	Magnetic volume fraction	Solid volume fraction	Conversion parameter	Non-magnetic fraction	Non-magnetic layer thickness
	$\varepsilon_M$ [ % ]	$\varepsilon_S$ [ % ]	$\gamma$	$\Delta\varepsilon$ [ % ]	$2a$ [nm]
L <sub>1</sub>	0.48	0.79	0.609	0.309	1.6705
L <sub>2</sub>	1.35	2.28	0.592	0.929	1.6847
L <sub>3</sub>	3.11	5.92	0.525	2.813	1.6799

From Table 4.2 it can be seen that the conversion parameter has sub-unitary values ( $\gamma < 1$ ) because the solid volume fraction is greater than the magnetic volume fraction :  $\varepsilon_S > \varepsilon_M$  [67].

The ratio  $\varepsilon_M/\varepsilon_S$  shows that a large fraction of the solid matter in suspension is not magnetic, the main reason for this being the non-magnetic layer on the surface of the particles. The non-magnetic fraction is given by subtracting the volume fractions  $\Delta\varepsilon = \varepsilon_S - \varepsilon_M$ .

A smaller value of the conversion parameter is primarily determined by the non-magnetic fraction ( $\Delta\varepsilon$ ) contained by the magnetic particles. If the parameter ( $\gamma$ ) has a very small value, the presence of agglomerates is not excluded [68].

The values obtained by other authors [69] indicate that the parameter  $\gamma$  may have values within the range ( $0.3 < \gamma < 0.8$ ) while the average values of  $\gamma$  calculated in this study for samples L1, L2 and L3 is within the range ( $0.525 < \gamma < 0.609$ ).

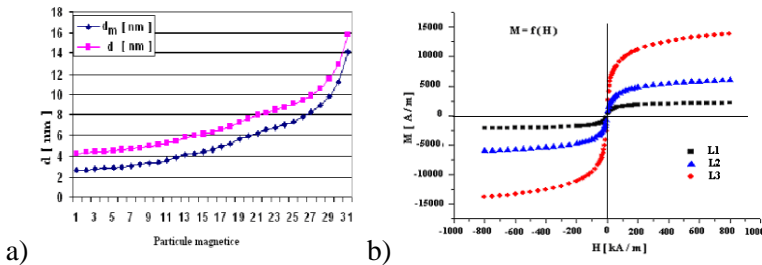


Fig. 4.4. a) Physic and magnetic diameter subtraction variation expressed through the thickness of the non-magnetic layer.  
b) Complete magnetization curves for samples L1, L2 and L3.

In fig.4.4 a) the non-magnetic layer thickness has the same value, regardless of particle size, for a given magnetic fluid. So it does not depend on diameter, it only depends on the nature of the substance.

Figure 4.4.b confirms the influence of the stabilizer on the shape of the magnetization curve. It reduces the interactions between particles and contributes to the decrease of the magnetization curve area until it becomes linear, as shown in Figure 4.4 where the complete curves have no hysteresis (the studied nanofluids have a superparamagnetic behavior).

### 4.1.3. Study of the magnetic properties by analyzing the magnetization curves

This study looked particularly at the following aspects:

- a) Description of the samples using magnetic measurements and the superparamagnetic behavior analysis of these samples.
- b) Magneto-granulometric analysis of the magnetization curves.

a) Description of nanofluid samples based on the magnetic measurements performed using the VSM 880 vibrating sample magnetometer. The static magnetization curves at room temperature for the petroleum based magnetic nanofluid samples L1 and L3 with the solid volume fraction  $\varepsilon_{S1} = 0.79\%$  (L1) and  $\varepsilon_{S3} = 5.92\%$  (L3) were drawn. The same was done for the kerosene based sample L2 which has the volume fraction of dispersed solid  $\varepsilon_{S2} = 2.28\%$  (L2).

Figure 4.5.a shows the initial magnetization curves.

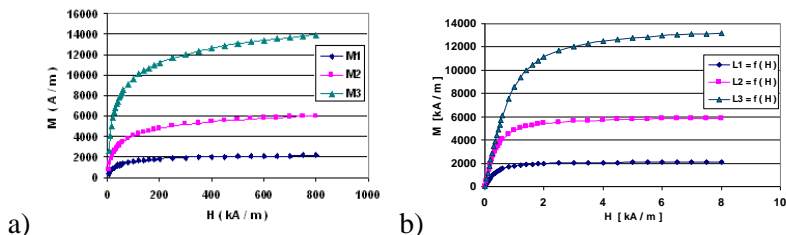


Fig.4.5. a) Curbele de magnetizare pentru probele L1, L2 și L3.  
 b) Curbele de magnetizare  $M = f(H)$  de tip Langevin.

The curves depicted in Figure 4.5.a show that the magnetization follows a Langevin type law that allows the study of

the superparamagnetic behavior of the samples. For this purpose the experimental data of the samples were fitted with a Langevin equation to obtain the theoretical magnetization curves (as seen in Figure 4.5.b) [70].

Other parameters were also determined: average magnetic diameter ( $d_m$ ), particle concentration ( $n$ ), magnetic volume ( $V_m$ ). The results are shown in Table 4.3.

The location of experimental points on these curves and the decrease of magnetic susceptibility confirms that samples L1, L2 and L3 have a superparamagnetic behavior [71].

Table 4.3. Parameters determined by analyzing the magnetization curves.

Sample	$M_S$ [kA/m]	$H_0$ [kA/m]	$d_m$ $10^{-9}$ [m]	$V_m$ $10^{-25}$ [m <sup>3</sup> ]	$n$ $10^{23}$ [m <sup>-3</sup> ]	$\chi_i$
L1 (0.79 %)	2154	487.38	3.071	0.1516	3.185	0.071
L2 (2.28 %)	6017	554.44	2.942	0.1333	10.121	0.158
L3 (5.52%)	13870	555.34	2.941	0.1331	23.368	0.531

As data presented in Table 4.3 shows, for the volume fractions of the studied magnetic nanofluids, the initial susceptibilities are smaller than those found in the scientific literature [72]. The magnetic susceptibility depends on the volume fraction  $\chi \sim \varepsilon_M$  and on the magnetic volume of particles  $\chi \sim V$ .

Figure 4.6.a shows the susceptibility dependence of sample L1, L2 and L3 on the magnetic field intensity  $\chi = f(H)$  [73].

The most significant decrease in susceptibility happens to sample L3. As the magnetic field's intensity increases from zero with  $\Delta H = 0.5 \cdot 10^5 A/m$ , susceptibility's initial value of ( $\chi_{3i} = 0.531$ ) decreases towards  $\chi = 0.1$ . As earlier mentioned, the decrease of magnetic susceptibility during the magnetization process of the samples, confirms that all three magnetic nanofluid samples have a superparamagnetic behavior [74].

Figure 4.6.b simultaneous presents the evolution of the magnetization and susceptibility for the same sample of magnetic nanofluid. It can be seen that the magnetization increases as the magnetic susceptibility of the sample decreases during the magnetization process [75, 76].

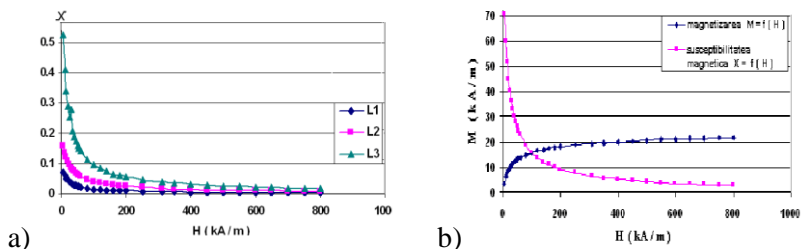


Fig.4.6 a) Magnetic susceptibility's dependence on magnetic field intensity . b) Magnetic susceptibility and magnetization dependence on the intensity of the magnetic field  $M = f ( H )$  și  $\chi = f ( H )$ .

To analyze the effect of the interactions between particles on the reduced magnetization curves, a qualitative study has been conducted which involved overlapping the curves and interpreting the results.

Figure 4.7.a shows a very good overlap of the reduced magnetization curves obtained from experimental results [77, 78].

Figure 4.7.b shows the reduced magnetization curves obtained from the Langevin model, for samples L1, L2 and L3.

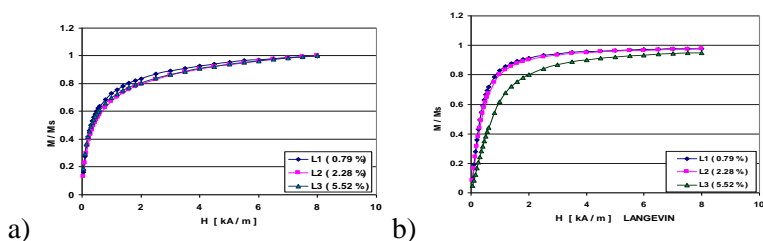


Fig. 4.7 a) The reduced magnetization curves experimentally obtained. b) The reduced magnetization curves obtained from the Langevin model for samples L1, L2 and L3.

For samples L1 and L2 we can see a very good overlap in low magnetic fields, which indicates a behavior consistent with Langevin descriptions. The particles in these magnetic nanofluids are double-coated with oleic acid which makes the interaction between them to be negligible [79, 80].

The interaction influence is noticeable in sample L3 and we do not rule out the presence of agglomerates that widen the

dimensional distribution in the large particle region and cause an increase of the initial susceptibility ( $\chi_{3i} = 0.531$ ). Comparing the reduced curves in Figure 4.7.a and 4.7.b it is found that the influence of particle interactions on the scale of the entire curve is difficult to reveal (it is apparent only in very weak fields) [81].

b) Magneto-granulometric analysis of the magnetization curves.

In order to determine the dimensional distribution parameters ( $D_0$ ) and (S), the average magnetic diameter ( $d_m$ ) and standard deviation ( $\sigma$ ), the values of Ms, H and  $\chi$  were extracted from Table 4.3 and for mathematical calculation a specialized computer program for numerically solving equations was created in Delphi programming language [82].

Table 4.4. Calculated values for the dimensional distribution parameters of the particles [83, 84].

Calculated values		Minimum diameter	Medium diameter	Maxim diameter	Lognormal distribution parameter	Standard deviation
Sample	$\chi_{iL}$ Langevin	$D_0$ [nm]	$\langle D_m \rangle$ [ nm ]	D [nm ]	S	$\sigma$ [ nm ]
L1	0.072	3.071	6.53	11.13	0.654	2.729
L2	0.167	2.43	5.99	10.36	0.678	2.392
L3	0.645	2.941	7.72	11.74	0.679	4.317

#### 4.1.4. Influence of magnetic material on the geometry of the magnetic field lines.

Analyzing Figure 4.9 it is possible to explain the processes that occur in the studied samples L1, L2 and L3 while measurements in magnetic field are conducted. The particle's magnetic moments have oriented in the direction of the field lines causing the magnetization process of the samples.

The magnetic susceptibility decreased more at low values of the field  $H < 0.5 \cdot 10^5$  A/m, the magnetic permeability also decreased in accordance with the equation  $\mu_r = (1 + \chi)$  and the magnetic induction increase corresponds to the interior field induction ( $B_i$ ) of the magnetic particles.

Figure 4.9.b shows how the magnetic permeability decreases ( $\mu$ ) while the magnetic field induction increases ( $B$ ). The relative magnetic permeability does not stay constant during the magnetization of the sample because it varies with the magnetic susceptibility  $\mu_r = f(\chi)$  [85-91].

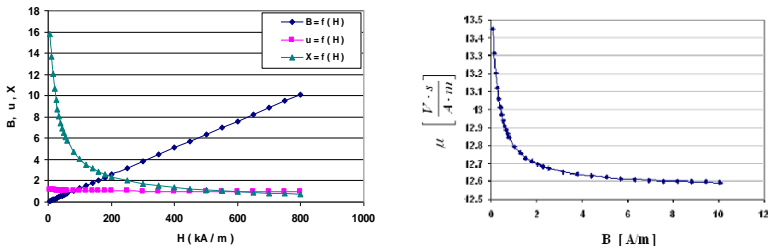


Fig.4.9.a) Parameters  $B$ ,  $\mu$ ,  $\chi$  dependence on the magnetic field intensity. b) Relative magnetic permeability dependence on the increase of the magnetic induction ( $B$ ).

#### 4.1.6. Determining the magnetic susceptibility through Gouy's method.

Quasi-static magnetic measurements were performed on magnetic nanofluids L1, L2 and L3 through Gouy's method over a period of several years.

In the first step we obtained the magnetization curves for cylindrical samples suspended in a perpendicular magnetic field. We have conducted three sets of measurements for each distance between the electromagnet poles as follows:  $d_1= 94$  mm,  $d_2= 50$  mm and  $d_3= 35$  mm. Some of the results are shown in Figures 4.10.a and 4.10.b [92, 93].

The second step was to conduct the measurements again two years later to study the stability over time and we concluded that the magnetic nanofluid samples were homogeneous and stable. Saturation magnetization values are in good agreement with recent results published by other authors (corresponding to the small volume fraction  $\varepsilon < 0.16$ ) [94].

The third step was to obtain the magnetization curves at low temperatures (243 K) with an original installation developed in the laboratory of the Faculty of Mines in Petrosani [95].

From the data shown in Figures 4.10.a and 4.10.b it can be seen that the values of the initial susceptibility and those of the sample's magnetization are not the same as before, when the distance between the polar pieces of the electromagnet is reduced and the measurements retaken.

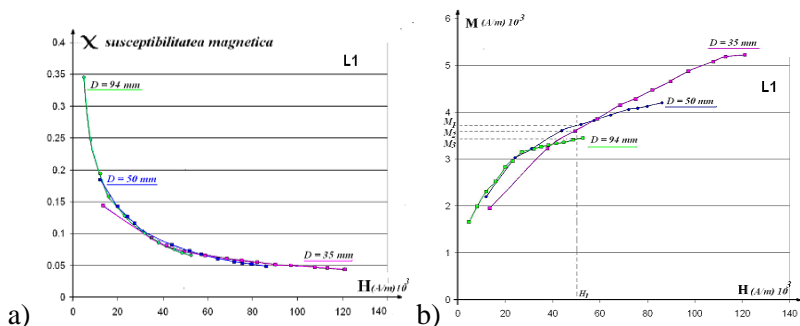


Fig.4.10.a) Susceptibility dependence on the intensity of the field.  
 b) Magnetization dependence on the intensity of the magnetic field

$$\chi_1 = f(H) \quad \text{and} \quad M_1 = f(H) \quad \text{for sample L1.}$$

Regarding the third step of the study, for measurements at low temperatures ( $T=243$  K) and at room temperature ( $T=300$  K) we found that the saturation magnetization increases as the temperature decreases. The lognormal distribution functions of particles diameter were remade and it was observed that at low temperatures, the average size of particles diameter is larger and the particles diameter dispersion is smaller.

*The influence of temperature on the stability on samples* is displayed in Figure 4.11.a where the thermal energy, volume and particle position based on temperature are all displayed. This influences the density and viscosity of the base liquid. At very low temperature, Kerosene has the density  $\rho = 0.853 \cdot 10^3 \text{ kg/m}^3$ , the cinematic viscosity  $\eta_c = 6.5 \cdot 10^{-6} \text{ m}^2/\text{s}$  and dynamic viscosity  $\eta_d = 5,53 \cdot 10^{-3} \text{ kg/ms}$ . Under these conditions, Kerosene tends to become a gel, denser and more viscous, it can hold very large particles ( $d = 548,7 \text{ nm}$ ) in suspension. The thermal energy of the particle has the value  $W_T = 3.35 \cdot 10^{-21} \text{ J}$  at a low thermal agitation.

Figure 4.11.b shows that at low temperatures ( $T=243\text{ K}$ ) the maximum size of the particles has a high value ( $d = 5.49 \cdot 10^{-7}\text{ m}$ ) due to the thick (viscous) environment that can maintain large particles (even dimensions of  $10^{-6}\text{ m}$ ) in suspension. As the temperature increases, so does the fluidity of the environment due to the decrease of its viscosity and the thermal motion intensifies [96, 97].

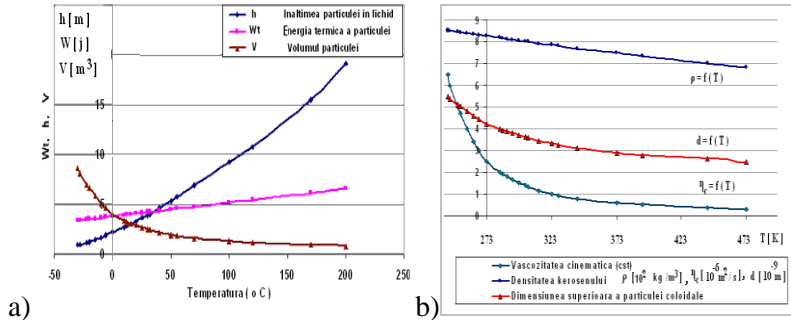


Fig.4.11.a) The influence of temperature on the position of the particle (h) in the fluid, on the thermal energy and particle volume. b) Particle's viscosity, density and maximum size dependence on temperature.

#### 4.2.1. Study on the stability of magnetic nanofluids in gravitational field.

It has been experimentally found that the magnetic nanofluids in samples L1, L2 and L3 can hold in suspension, without the issue of gravitational sedimentation, particles with a maximum size of  $d = 347\text{ nm}$ .

Observations and measurements revealed that the particle dimensions (diameter, volume and radius) affect their vertical distribution inside the fluid [98].

L2 magnetic nanofluid sample contains particles with large volumes ( $V = 39.47 \cdot 10^{-25}\text{ m}^3$ ) and are found at  $h_2$  height ( $h_2 = 2.43 \cdot 10^{-2}\text{ m}$ ) which is less than the height where particles are found in the other two samples ( $h_1 = 3.4 \cdot 10^{-2}\text{ m}$  and  $h_3 = 3.79 \cdot 10^{-2}\text{ m}$ ). The magnetic nanofluid's height in the vessel must be sufficiently small (in the order of  $10^{-2}\text{ m}$ ) so as to avoid the gravitational sedimentation of particles.

The sedimentation rates calculated for the magnetic particles contained in our studied samples are:  $v_1 = 0.52 \cdot 10^{-6}$  m/s (L1),  $v_2 = 0.66 \cdot 10^{-6}$  m/s (L2) and  $v_3 = 0.49 \cdot 10^{-6}$  m/s (L3). It is noted that the small particles of sample L3 have a lower sedimentation rate as their height is easily maintained by thermal agitation.

As seen, the sedimentation rates are in the order of  $10^{-6}$  m/s but in practice, rates  $10^3$  times greater are required for sedimentation to occur, so the studied samples do not suffer sedimentation in gravitational field [99].

Figure 4.12.a shows how the heights where particles are found in the liquid decreases with the increase of their volume  $h = f(V)$ .

Figure 4.12.b shows how particles with very small diameters ( $d < 5$  nm) may be in equilibrium over a period of time ( $t = 2.79$  months). This time period significantly decreases for particles with larger diameters ( $d > 10$  nm).

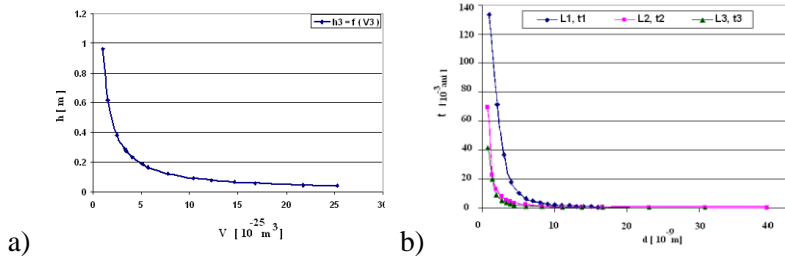


Fig. 4.12.a) Magnetic particle's position dependence on the volume  $h = f(V)$   
 b) The dependence of the time period in which the particles do not settle on the hydrodynamic diameter of the particles in L1, L2 and L3.

#### 4.2.2. Study on the stability of magnetic nanofluids in magnetic field.

The stability of the analyzed samples in magnetic fields requires that the solid particles suspended in the base liquid do not agglomerate and do not settle under the action of magnetic forces.

The dimensions of the magnetic particles used to prepare the studied samples are sufficiently small (3,34 – 19, 61 nm) so that each individual particle represents, from a magnetic point of view, a Weiss mono-domain with permanent magnetic moment [100].

We determined the magnetic moments of particles with values between the minimum ( $m_3= 0.1066 \cdot 10^{-20} \text{Am}^2$ ) and maximum value ( $m_2=134.45 \cdot 10^{-20} \text{A m}^2$ ).

Figure 4.13 shows that L2 nanofluid sample contains particles with greater magnetic moments than those of L1 and L3, meaning that it contains very large particles in its composition.

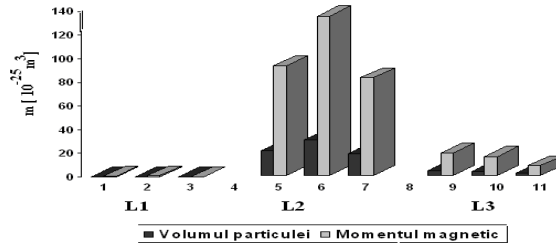


Fig.4.13. The magnetic moment's dependence on particle volume.

A magnetic sedimentation rate has been determined considering a magnetic field gradient of  $10^8 \text{ A/m}^2$ , the spontaneous magnetization of magnetite  $M_p = 4.46 \cdot 10^5 \text{ A/m}$ , environment's viscosity  $\eta=1.4 \cdot 10^{-6} \text{ m}^2/\text{s}$  and the magnetic permeability of vacuum  $\mu_0=12.56 \cdot 10^{-7} \text{ H/m}$ . The values calculated for the magnetic sedimentation rate are as follows:  $v_1= 444.58 \cdot 10^{-6} \text{ m/s}$  for sample L1,  $v_2 = 163 \cdot 10^{-6} \text{ m/s}$  for sample L2 and  $v_3=15 \cdot 10^{-6} \text{ m/s}$  for sample L3. The thermal energy ( $W_T = 0.414 \cdot 10^{-20} \text{ j}$ ) and magnetic dipole-dipole energy ( $W_{dd}$ ) of the particles in the range (0.00497–6.276)  $10^{-20} \text{ j}$  was calculated.

In order to avoid the magnetic induced agglomerates it is necessary that the magnetic dipole-dipole energy is smaller than the thermal agitation energy ( $W_{dd} < W_T$ ) [101].

### 4.3. The study of magnetic fluid viscosity in the absence of magnetic fields

In order to perform a study on the rheological behavior of L1, L2 and L3 samples at room temperature we used a Physica MCR 300 rheometer. The dependence of the viscosity ( $\eta$ ) and shear tension ( $\tau$ ) on the shear rate was shown and a linear dependence of the shear tension on the shear rate ( $\dot{\gamma}$ ) is observed.

Figures 4.14.a, 4.14.b and 4.14.c show that for L1 sample, the viscosity's value decreases on the first portion of shear rates interval then it remains constant. The sample has a non-Newtonian behavior indicating the presence of agglomerates in the fluid. For L2 and L3 samples the value of viscosity can be considered constant and these magnetic nanofluids have a Newtonian behavior over the investigated range of share rates [102-107].

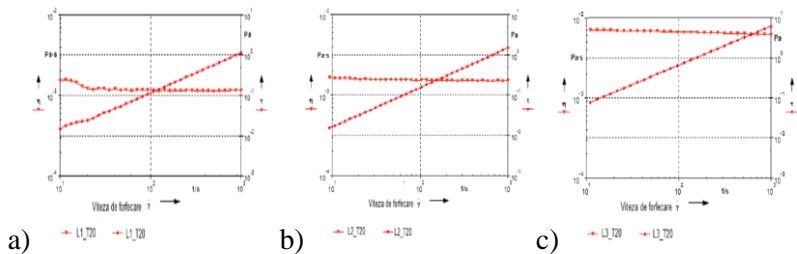


Fig.4.14. Viscosity's dependence on share rates for the magnetic nanofluid samples L1( a), L2 (b) și L3 (c).

Figure 4.15.a, 4.15.b and 4.15.c show the dependence of viscosity ( $\eta$ ) and shear tension ( $\tau$ ) on the share rate at different temperatures. As the temperature increases from 20°C to 60°C, viscosity decreases.

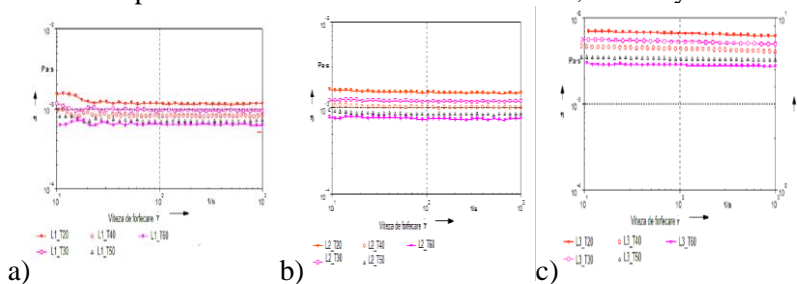


Fig.4.15 Viscosity's dependence on temperature for magnetic nanofluid samples: L1( a), L2 (b) and L3 (c).

#### 4.4. Possible applications of magnetic nanofluids. The magnetic nanofluid separation.

Nanoparticles with magnetic properties and magnetic nanofluids are extensively researched [108] in specific areas like industrial applications such as: magnetic separation of materials [109], toxic substances or bio-molecules ; magneto-rheological nanofluids for shock absorption [110]; nonlinear optical materials, optical switches and magnetically controlled optical modulators [111]; soft / hard nanostructured magnets [112]; loudspeaker [113]; chemical sensors for the detection of substances or magnetic fields [114]; data storage elements of very high density [115]; cooling fluids or heat exchangers [116,117]; wavelength filters magneto-optically controlled [118]; sealants [119]; bio-medical fluids with contrast agent applications [120,121]; hyperthermia [122,123]; bio-molecules or drugs carriers [124] or diagnosis and treatment elements [125-128].

By using the magnetic nanofluid separation method it is possible to develop non-polluting, economical and unconventional separation technologies. This idea highlights how the levitation technique can be used to recycle the non-ferrous waste left in broken light bulbs or fluorescent tubes. This separation would take place after a regular dry magnetic separation and would remove the non-magnetic material left. A magnetic nanofluid separator is shown in Figure 4.16.

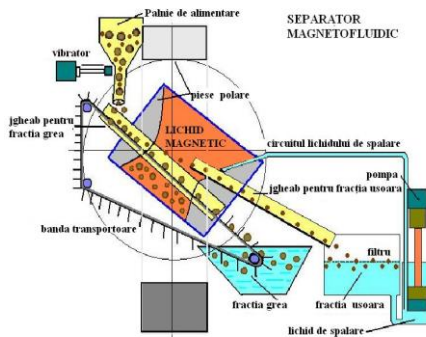


Fig. 4.16 Magnetic nanofluid separator type *SEB-650*.

The working parameters are as follows: the useful volume of the separation cell (0.8 – 1) liter; the saturation magnetization of the magnetic nanofluid is (250 – 330) GS and the induced magnetization of the magnetic nanofluid is (125-150) GS; the apparent density of the separation environment is (2300 -2700) kg /m<sup>3</sup>. The wet material is subject to separation inside a cell with a useful volume of 1 liter and using petroleum based magnetic fluid.

Metallic fractions (heavy) are collected at the bottom of the separation cell and ore fractions (light) levitate at the surface of the magnetic nanofluid and are collected at the top of the cell. The quantity of water adhering to the surface of separated material granules is 150 kg / tone.

The recovery of the magnetic nanofluid (from the surface of the separated material or mechanically driven) is done after a 30 minutes decantation period in the vessel where separated material is collected while the magnetic fluid is returned to the separation cells [129]. In order to increase the efficiency of the magnetic nanofluid separation method it is necessary to keep in mind some observations:

a) It has been observed that by moistening the raw material before the magnetic nanofluid separation reduces the quantity of adhered magnetic nanofluid by up to 55% [130].

b) To ensure the efficiency of this separation method it is mandatory to recover the magnetic nanofluid left on the separated fractions. These will be washed with petroleum and the newly obtained magnetic fluid (very diluted) will be used (after a purification process) as a solvent for diluting other magnetic fluids. In this way, the losses of magnetic nanofluid are reduced to a minimum of 0.1%.

## References (summary)

- [1]. Vonsovski S.V., *Magnetismul*, Ed. Științifică și Enciclopedică, București, 1086–1097 (1981).
- [2]. **Chioran V.**, *Fizica straturilor subțiri*, Revista de fizică” Cygnus” Ed “Cygnus” Unesco, Suceava, nr.2(4) 10-12, (2005).
- [3]. Blundell S., *Magnetism in Condensed Matter*, University of Oxford, Dep.of Physics, 12 (2001)
- [4]. **Chioran V.**, *Magnetizarea particulelor mici*, Rev.” Evrika” 12 (2012).
- [8]. Mansuripur M., *The Physical Principles of Magneto-optical Recording*, Cambridge University Press, 46 (1995).
- [9]. Doniga A. Vasilescu E., Buletinul AGIR, 105-107 (2012).
- [11]. **Chioran V.**, *Steric repulsion*, 14<sup>th</sup> National Conference of the Physics Romanian Physical Society, 13 -17 sept. Constanța, P 33 (2005).
- [13]. Davies K.J., Welss S., J.Mag. Mag. Mater, (122), 24-28 (1993)
- [15]. Vekilov P. G., *Gibbs, Volmer, and Crystal Nucleation* International School of Physics “Enrico Fermi” “Physics of Complex Colloids” Varenna, Lake Como, July 3 - 13, (2012).
- [17]. Wenn F., Zhang F., Zheng H., J. Mag. Mag. Mater. (324) 2471 (2012)
- [18]. Lukashevich M.V., J.Mag. Mag. Mater., (85), 216-218 (1990).
- [21]. Sedlacik M., Moucka R., Kozakova Z., Kazantseva N.E., Pavlinek V., Kuritka I., Kaman O., Peer P., J. Mag. Mag. Mater., (326), 7-13 (2013).
- [22]. Ludwig F., Remmer H., Kuhlmann C., Wawrzik T., Arami H., Ferguson R.M., Krishnan K.M, J. Mag. Mag. Mater., (360), 169-173 (2014).
- [23]. Widanarto W., Sahar M. R., Ghoshal S.K., Arifin R., Rohani M.S., Hamzah K., J.Mag.Mag. Mater., (326), 123-128 (2013).
- [24]. Nanjundappa C.E., Prakash N., J.Mag. Mag.Mater.,(370) 140 (2014).
- [26]. Krichler M., Odenbach S., J. Mag. Mag. Mater., (326), 85-90 (2013).
- [27]. Kúdelčík J., Bury P., Drga J., J.Mag.Mag.Mater (326), 75 (2013).
- [28]. Luca E., Călugăru Gh, Bădescu R., Bădescu V., Cotaș C., *Ferofluidede și aplicațiile lor în industrie*, Ed. Tehnică, București, 66- 71 (1978).
- [29]. **Chioran V.**, Micu F. *Ferofluidede, materiale ale viitorului*, Colocviul Național de Fizică,, Evrika -Cygnus” 7-9 septembrie Suceava (2007).
- [30]. Vaidyanathan I, Physica B:Condensed Matter, 403, (13), 2157 (2008).
- [32]. Naseri G., H., Saion.B., ,J.Mag.Mag.Mater, 350,141(2014)
- [33]. Lima R.S., Moura K., Physica B: Condens.Matter, 407(16) 3196 (2012) [35]. Zheng Y., Cheng Y., Bao F., Mater. Res. Bull. ,(41) 525-529 (2006).
- [36]. Brice B., Popa G., Fleutot S., Pichon B., Garofalo A., Ghobril C., Billotey C., Begin-Colin S Dalton Transactions (42), 2146 (2013).
- [37]. Shannigrahi S.R., Pramoda K.P. J. Mag.Mag.Mater.(324)140 (2012).
- [38]. Yue Z., Zhou J., Li L., Gui Z., ,J. Mag. Mag. Mater., (208),55 (2000).
- [40]. Sperlring R., Parak W., Phil. Trans. R. Soc. A 368, 1333 (2010).

- [42]. Laurent S., Forge D., Port M., Roch A., *Rev.* 108 (6), 2064 (2008).
- [46]. Faraji M., Yamini Y., Rezaee M., Iran J., *Chem. Soc.*, (7), 175 (2010).
- [49]. Kwon W.H., Lee J-G., Chae K.P., *Journal of Magnetism*, 18 (1) 26 (2013).
- [50]. Biasi S., Cardoso L.G., *Physica B: Condensed Matter*, 407(18) (2012).
- [51]. **Chioran V.**, Stanci A., *Utilization the gamma radiation in density of liquids measurement*, Simpoz. Internațional „UNIVERSITARIA SIMPRO” 2010, Petroșani, 35-36, (2010).
- [52]. **Chioran V.**, Ardelean I., Stanci A. - *The measurement of the magnetic susceptibility and of the magnetization using the Gouy method*, Proceeding of the International Balkan Workshop on Applied Physics, IBWAP2008, 7-9 iulie, Constanța, Ovidius University Press, 88 (2008).
- [53]. **Chioran V.**, Ardelean I., Stanci A., - *The measurement of the magnetic susceptibility and of the magnetization using the Gouy method* 15<sup>th</sup> National Conference of the Physics Romanian Physical Society, 10-13 septembrie, București, 168 (2008).
- [54]. **Chioran V.** Ardelean I., *Revista Fizică și Tehnologiile Moderne*, Societatea Fizicienilor din Moldova, Chișinău, (7) 3-4 (2009).
- [55]. P.C. Fannin, *J. Mag. Mag. Mater.* 252 (2002).
- [56]. **Chioran V.**, *Revista Fizică și Tehnologiile Moderne*, Societatea Fizicienilor din Moldova, Chișinău, nr.3 -4 (2) 48 (2004).
- [60]. **Chioran V.**, *Fizica straturilor subțiri*, Fizica și Tehnologiile Moderne, Societatea Fizicienilor din Moldova, Chișinău, 1-2 (3) (2005).
- [61]. Mackay M. E., Tuteja A., Duxbury P. M., Hawker C. J., Van Horn B., Guan Z., Chen G., Krishnan R. S., *Science*, (311), 1740 (2006).
- [62]. **Chioran V.**, Micu F. - *Repulsia sterică a ferofluidelor*, Conferința Fizicienilor din Moldova 2007, Chișinău, 22 (2007).
- [63]. Lee W-K., Ilavsky J., *J. Mag. Mag. Mater.*, (330), 31-36 (2013).
- [64]. **Chioran V.**, Micu F., *Cât de magnetic poate fi un fluid magnetic?* Conferința Fizicienilor din Moldova 2007, Chișinău, 20 (2007).
- [65]. **Chioran V.**, Chioran M., *Methods for Determining the Quality of Magnetic Fluids* *Journal of Magnetism*, Korea, 18(2), 197-201 (2013).
- [66]. **Chioran V.**, Aurora Stanci A., Stanci A\*, Chioran D., -*Methods for Determining the Quality and Stability of Magnetic Fluids*, The 17<sup>th</sup> International Conference The Knowledge-Based Organization, Conference Proceedings 3 Applied Technical Sciences and Advanced Military Technologies, Sibiu, 236-239, (2011). în curs de indexare ISI,
- [67]. **Chioran V.**, Ardelean I., Stanci A., Chioran D. - *Determining the quality of the magnetic fluids using of conversion parameter of the magnetic properties*, Proceeding of the International Balkan Workshop on Applied Physics, IBWAP2011, 6-8 iulie 2011, Constanța, România, Ovidius University Press, 148 (2011).

- [68]. **Chioran V.**, Stanci A., Ardelean I., Chioran D., *Determining the quality of the magnetic fluids using of conversion parameter of the magnetic properties* Colocviul Național "Eureka -Cygnus" Bușteni (2011).
- [70]. Williams H., O'Grady K., Chantrell .W., *J.Mag.Mag.Mater.* 122 (1993).
- [71]. Ledermann M., Schultz S., Ozaky M., *Phys. Rev. Lett.*(73),986 (1994).
- [77]. Hrianca I., Malaescu I., *J. Magn. Magn. Mater.*, (150), 131(1995).
- [78]. Jung H-S., Hong Y. K., *IEEE Trans. Magn.*, (34), 1675 (1998).
- [79]. Fannian P., Charles S. W.J. *Magn. Magn. Mater.*,(201), 98 (1999).
- [82]. **Chioran V.**, Todoran R., *Interactive Learning of Physics*, 12<sup>th</sup> National Conference of the Physics Romanian Physical Society" Trends in Physics"26-28 sept. ed.Petru Maior" University, Târgu Mureș 115 (2002).
- [83]. Phromsuwan U., Sirisathitkul C., Sirisathitkul Y., Uyyanonvara B., Muneesawang P., *Journal of Magnetism*, 18 (3) 311-316 (2013).
- [84]. **Chioran V.**, Chioran M., *Caract.nanofluidelor magnetice, analiza magnetogranulometrică*, Col. Naț."Eureka -Cygnus"31aug.Constanța (2012)
- [85]. He L., et. al., *J. Magn. Magn. Mater.*, (155), 6 (1996).
- [87]. Hrianca I., Malaescu I., *J.Mag. Mag. Mater.* 150 (1995).
- [88]. Malaescu I., Gabor L., Stefu N., *J. Mag. Mag. Mater.* 222 (2000).
- [90]. Yu.P. Kalmykov, W.T. *Phys. Rev. B*, 56 (6) (1997).
- [91]. Xu H., Wang C., Ma X., Li Y, Liu Z., *Biomaterials* 32, 9364 (2011).
- [92]. **Chioran V.** Ardelean I, *Revista Fizica și Tehnologiile Moderne, Societatea Fizicienilor din Moldova, Chișinău*, (8) 1-2 (2010).
- [93]. **Chioran V.**, Ardelean I., Stanci A., *Buletinul GIIF (Grupul de Inițiativă pentru Învățarea Fizicii), Călărași*, (1) 28 (2008).
- [94]. **Chioran V.**, Stanci A., Micu F., *Măsurarea susceptibilității magnetice și a magnetizației folosind metoda Gouy*, Colocviul Național de Fizică "Eureka -Cygnus" 5-7 sept. Suceava (2008).
- [95]. **Chioran V.**, Ardelean I ; *Revista Științifică "V Adamachi"* (1) 5(2008)
- [96]. **Chioran V.**, Chioran M., *Revista „Eureka” Brăila*, nr.7-8, 76, (2013).
- [97]. **Chioran V.**, Chioran D., *Studiu asupra proprietăților fizice ale ferofluidelor*, Colocviul Național "Eureka -Cygnus" 6 sept. Ploiești (2013).
- [98]. **Chioran V.**, *Stabilitatea fluidelor magnet. Rev.*, "Eureka" Brăila, 6 (2011)
- [99]. **Chioran V.**, Chioran D., *„Metode de studiu a stabilității fluidelor magnetice* Colocviul Național "Eureka Cygnus"5 sept., Tulcea (2010).
- [100]. **Chioran V.**, Chioran D., Micu F., *Revista de Fizică" Cygnus" Ed. "Cygnus" Unesco, Suceava*, nr.2 (13) 39 - 42, (2010).
- [102]. Vekaș L. Bica D., *J. Coll. Int.*, 231, 247 (2000).
- [103]. Resiga D., Vekaș L., *Comportarea reologică a fluidelor magnetizabile* Ed. Orizonturi universitare, Timișoara, 15 (2002)
- [104]. **Chioran V.**, Ardelean I., Chioran D., *Verificarea relației lui Arhenius la ferofluid* Colocviul Național de Fizică "Eureka -Cygnus"4-9 septembrie, Suceava (2009).

- [105]. **Chioran V.**, Chioran D., *Determinarea curbilor de curgere pentru ferrofluide* Colocviul Național “Evrika -Cygnus” 3-5 sept., Tulcea (2010).
- [108]. Taylor R., Coulombe S., Otanicar T., Phelan P., Rosengarten G., Prasher R., Tyagi H., *Journal of Applied Physics* 113, 011301 (2013).
- [109]. **Chioran V.**, Ardelean I., *The Recovery of Non-ferrous Metals from Broken Light Bulbs using the Magnetic Liquid Based Separation*, Journal of Magnetism, The Korean Magnetism Society, 15(2), 91-98 (2010).
- [110] Jan Svoboda - *Magnetic techniques for the treatment of materials Advances in Global Change Research Series*, Springer, (2004), 227-240.
- [111]. Morjan I., Dumitrache F., Soare I., Dutu I. E., Filoti G., Prodan G., Popa N. C., Vékás L., *Advanced Powder Technology*, 23, 88 (2012).
- [112]. Akman O., Kavas H., Baykal A. J. *Mag. Mag. Mater.* (327) 151 (2013).
- [113]. Zhuonan L., Huihui Y., Laifeng L., *Cryogenics* 52, 699 (2012).
- [114]. Andrzej M., *Mechanical Systems and Signal Processing* 528 (2013).
- [115]. Poudyal N., Liu J. P., *J. Phys. D: Appl. Phys.* 46, 043001 (2013).
- [116]. Xiong C. L., Guang H. X., Hu Z. J., *Optics letters*, 36, 2761 (2011).
- [117]. Shin J., Thompson J., *Nanotechnology* 23 (15) 155602 (2012).
- [118]. Peyghambarzadeh S. M., Hashemabadi S. H., Hoseini S. M., Seifi J., *International Communications in Heat and Mass Transfer* 38, 1283 (2011).
- [119]. Huminic G., *Experiment. Thermal and Fluid Science* (35) 550 (2011)
- [120]. Kleinstreuer C., Feng Y., *Nanoscale Res. Lett.* 6(1), 229 (2011).
- [122] Landi G. T., *J. Mag. Mag. Mater* (326), 14–21 (2013).
- [123]. Borbáth T., Bica D., Potencz I., Vékás L., Borbáth I., *Conference Series: Earth and Environmental Science* 12 (1), p.012105 (2010).
- [124]. Hosseini F., Panahifar A., Adeli M., Amiri H., Lascialfari A., Orsini F., Doschak MR., *Colloids Surf B Biointerfaces* 103, 652 (2013).
- [126]. Franke K., Kettering M., Lange K., Kaiser W., Hilger I., *International journal of nanomedicine* 8, 351 (2013).
- [127]. Chaturbedy P., Chatterjee S., Selvi R. B., Bhat A., Kavitha M. K., Tiwari V., Patel A. B., Kundu T. K., Maji T., Eswaramoorthy K. M., *J. Mater. Chem. B* 1, 939 (2013).
- [128]. Wan Q., Xie L., Gao L., Wang Z., Nan X., Lei H., Long X., Zhi-Ying Chen, C.-Yi He, Liu G., Liu X., Qiu B., *Nanoscale* 5, 744 (2013).
- [129]. Stanci A., **Chioran V.**, Stanci A\*, *The separation non-ferrous materials with spectrometer ferrofluidic of density*, The 17th International Conference The Knowledge-Based Organization, Conference Proceedings 3 Applied Technical Sciences and Advanced Military Technologies, ISSN 1843-6722, pg. 182-186, (în curs de indexare ISI), (2011).
- [130]. **Chioran V.**, Stanci A., Suzana A., *Recovery of non-ferrous metals from waste electrical using the magnetofluidic separation*, Proceedings of the 15th Conference of Environment and Mineral Processing Part I, Eds. Fečko & Čablik, VSB-TU Ostrava, Czech Republic, 41-45, 2011,

## Conclusions

1. This thesis is focused on the study of the physical properties of some magnetic nanofluids. There are two main objectives that define the structure of this thesis: the preparation of magnetic nanofluids and the analysis of the obtained samples.

For the analysis of the samples we used different techniques and methods: structural analysis, sample quality analysis, study of the magnetic and rheological properties, study on the stability in gravitational and magnetic fields and study regarding the influence of temperature on the physical properties of nanofluids.

2. Three magnetic fluid samples called L1, L2 and L3 were prepared in the laboratory. In their composition, these samples have mono-domain magnetite nanoparticles stabilized with oleic acid and dispersed in petroleum (samples L1 and L3) or kerosene (for sample L2). The saturation magnetization of the samples has values ranging between (2.154 - 13.870 kA/m) and the magnetic volume fraction corresponding to it has values ranging between (0.07 - 3.11 %).

3. It has been shown that the filamentary structure filtering method in magnetic field gradient followed by ultracentrifugation is better than the filtration in gravitational field. This method has been used for L3 sample and we found an increase in particle density and saturation magnetization. These parameters have the following values:  $M_{S3}=13.87$  kA/m,  $V_{m3}=0.133 \cdot 10^{-25} \text{m}^3$  and  $n=23.368 \cdot 10^{23} \text{m}^{-3}$ .

4. Having a sub-unitary value, the conversion parameter highlights the fact that a fraction of the solid matter in the suspension is not magnetic. This fact can be seen from the values obtained for the analyzed samples, where  $\Delta\varepsilon_1=0.3\%$  (L1),  $\Delta\varepsilon_2=0.93\%$  (L2) and  $\Delta\varepsilon_3=2.81\%$  (L3). The maximum values of the parameter are in the  $(0.729 < \gamma < 0.764)$  range which leads to the conclusion that magnetic nanofluids prepared in this way have the magnetic qualities required for their use in various applications.

5. The quasi-spherical shape of the particles and the magnetite's crystalline network type were observed by electron microscopy techniques. The electron diffraction images through diffraction rings confirm the sample's polycrystalline feature and crystallinity. Micrographs show a core-shell structure of the particles as well as their chain, fractal and mixed agglomeration tendency.

6. By analyzing the histograms and distribution curves of the particles it was confirmed that the samples contain particles with sizes in the order of  $10^{-9}$  m situated in a Gaussian dimensional distribution. The average magnetic diameters calculated for the studied samples are:  $d_{m1}= 9.32$  nm (L1),  $d_{m2}= 8.83$  nm (L2) and  $d_{m3}= 7.02$  nm (L3). In the analyzed samples, the smallest particles have magnetic diameter values in the (1.66-3.49 nm) range and the largest particles have magnetic diameters in the (7.93 - 15.23 nm) range.

7. The diameter of the magnetite particles contained in L1, L2 and L3 samples were directly determined by using electron microscopy techniques or by analyzing the magnetization curves. Between diameters there is certain dependence:  $d_{\text{magnetic}} < d_{\text{physic}} < d_{\text{hydrodynamic}}$  because  $d_{\text{magnetic}} = d_{\text{physic}} - 2a$  (for magnetite  $a=0.83$  nm) and  $d_{\text{hydrodynamic}} = d_{\text{physic}} + 2\delta$  (for oleic acid  $\delta = 0.86$  nm).

8. The thickness of the non-magnetic layer on the surface of magnetite particles was calculated and the average value obtained is  $a=0.839$  nm. It was found that the thickness of the non-magnetic layer is the same for all the magnetite particles in a sample, regardless of the physical diameter. This means that the volume of a small spherical particle contains a greater non-magnetic fraction than the volume of a large particle. For this reason, it can be said that the large particles are more “magnetic” than the small ones.

9. The superparamagnetic behavior of the magnetic particle systems in our nanofluid samples has been investigated. The results confirm this behavior, well described by a Langevin type equation.

10. We analyzed the factors determining the stability of magnetic nanofluids in gravitational field and observed:

a) the magnetite particles within the samples have much smaller dimensions than the maximum calculated dimension ( $d = 346.6$  nm);

b) the sedimentation rate in gravitational field has this value :  $v_s = 0.49 \cdot 10^{-6} \text{ m/s}$  , which is  $10^3$  times smaller than the real-life sedimentation rate value;

c) for the analyzed samples, the maximum height where small magnetic particles ( $V=25 \cdot 10^{-25} \text{ m}^3$ ) can be found at is  $h=3.79 \cdot 10^{-2}$  m and the length of time that the particles remain in equilibrium in the base liquid is around 2.79 months. It was found that the analyzed magnetic nanofluids are ultra-stable and have no tendency of sedimentation.

Am deosebita plăcere de a vă invita la  
susținerea publică a tezei de doctorat intitulată:

„Studiul proprietăților fizice ale unor  
nanofluide magnetice”

având drept conducător științific pe d-l Prof. Dr. Emerit  
Ioan Ardelean, în data de 30 septembrie 2014 la ora 11<sup>00</sup>  
în Amfiteatrul „Augustin Maior” al Facultății de Fizică

Viorica Chioran